Left Ventricular Cavity-to-Myocardium Count Ratio in Technetium-99m-Sestamibi SPECT in the Detection of Resting Left Ventricular Dysfunction

Roberto Sciagrà, Gianni Bisi, Piergiovanni Buonamici, Francesca Zerauschek, Giovanni M. Santoro, Ugo Meldolesi, Pier Filippo Fazzini and Alberto Pupi

Nuclear Medicine Unit, Department of Clinical Pathophysiology, University of Florence; and Division of Cardiology, Careggi Hospital, Florence, Italy

The aim of this study was to assess the value of the cavity-to-myocardium count ratio (C/M ratio) calculated in resting ^{99m}Tc-sestamibi SPECT images to identify patients with depressed left ventricular ejection fraction (LVEF). **Methods:** In the 95 patients studied, the C/M ratio was calculated from the midventricular short-axis slice using regions of interest drawn in the center of the cavity and in the most active area of the ventricular wall; its value was compared with LVEF measured using two-dimensional echocardiography. **Results:** The C/M ratio correlated with LVEF ($r = 0.6$, $p < 0.000001$) and was significantly lower in patients with abnormal LVEF than those with normal LVEF: 0.026 ± 0.028 versus 0.125 ± 0.093, $p < 0.000001$. In the entire patient population, a C/M ratio < 0.07 identified the patients with depressed LVEF with a 94% sensitivity, 71% specificity and 82% accuracy. **Conclusion:** The resting ^{99m}Tc-sestamibi C/M ratio is a useful parameter in identifying patients with depressed LVEF directly from the SPECT perfusion images.

Key Words: technetium-99m-sestamibi; left ventricular function; cavity-to-myocardium count ratio; SPECT

$\mathbf{A}$dvantages of ^{99m}Tc-sestamibi over ^{201}Tl for myocardial perfusion imaging include: (a) the optimum features it has for SPECT (1,2) and (b) the possibility of directly evaluating left ventricular function by collecting first-pass radionuclide angiography data during tracer injection or by acquisition of gated perfusion images (3–6). From ^{201}Tl perfusion studies, only indirect estimates of abnormal left ventricular function can be obtained. The best known and clinically valuable are the transient left ventricular dilation (7) and the increased lung uptake in post-stress images (8), which indicate the presence of severe coronary artery disease with exercise-induced left ventricular dysfunction. It should be noted, however, that with ^{99m}Tc-sestamibi, the presence of a stress-induced transient left ventricular dilation may be missed because of the delay between stress testing and image collection. The value of lung uptake in exercise ^{99m}Tc-sestamibi scintigraphy, as a sign of extensive coronary artery disease, was demonstrated using planar imaging (9), but a significant relationship with coronary angiographic findings was observed only in early poststress images (10). Furthermore, only a fair correlation was found between the ^{99m}Tc-sestamibi lung-to-heart count ratio (L/H ratio) and rest and stress left ventricular ejection fraction (LVEF) (11). Recently, the value of a low ^{201}Tl cavity-to-

myocardial count ratio (C/M ratio) to detect patients with resting left ventricular dysfunction has been demonstrated (12). This study aimed to verify the possibility of identifying resting left ventricular dysfunction by calculating the C/M ratio in baseline ^{99m}Tc-sestamibi SPECT images. In addition, the reliability of the C/M ratio was compared with that of the L/H ratio.

MATERIALS AND METHODS

Patients

The study group included 95 patients and was retrospectively selected from patients who had undergone resting ^{99m}Tc-sestamibi SPECT in our laboratory (74 men, 21 women; range 39–77 yr; mean age 569.8 ± 9.4 yr). SPECT images were acquired to define the baseline perfusion pattern in clinically stable patients with previous myocardial infarction or as part of a two-day rest-stress protocol, performed to detect the presence of coronary artery disease in patients with suspect chest pain. Patients with history or signs of heart disease other than coronary artery disease were excluded from the study, even if they had fulfilled the selection criteria. Patients were included in the study if a technically adequate echocardiogram performed within 1 wk of the scintigraphic examination, with the patient in stable clinical conditions, and with unchanged drug regimen was available, to allow a reliable measurement of the LVEF. The recorded two-dimensional echocardiograms of all eligible patients were reviewed to control quality in LVEF evaluation.

Two-Dimensional Echocardiography

An Aloka SSD-870 ecocardiograph with 2.5–3.5 MHz transducers was used. Patients were studied at rest in the left lateral decubitus position. For LVEF calculation, a monoplane area-length method was applied on three consecutive cardiac cycles examined with the apical four-chamber view, and the mean of the three measured values was used as LVEF (13,14). According to the current practice of our laboratory, the lower limit of normal LVEF was 50%. For all 95 enrolled patients, the echocardiographic images enabled an accurate measurement of the left ventricular end-diastolic diameter (LVEDD). The LVEDD was measured in a monodimensional mode using a freezed image acquired in the parasternal short- or long-axis sections, with the cursor at the level of the cordae tendinae (15). The mean of three repeated measurements was used.

Technetium-99m-Sestamibi Scintigraphy

SPECT was collected 60 min after ^{99m}Tc-sestamibi injection. A gamma camera equipped with a high-resolution collimator and a 20% window centered at the 140 keV photopeak of ^{99m}Tc was used. Sixty projections, 20 sec each, were acquired in step-and-shoot mode over a 180° arc, using a zooming factor 1.4 and 64 ×

64 matrices. The image reconstruction was performed with filtered backprojection using the combination of a ramp filter with a first order Hanning filter (cutoff frequency of 0.5 cycles/cm). No attenuation or scatter correction was used. The transaxial slices were realigned along the heart axis obtaining short-axis, vertical and horizontal long-axis slices.

C/M Ratio

The C/M ratio was calculated according to the procedure proposed by Roberti et al. (*12*). Briefly, a 2 × 2 pixel rectangular region of interest (ROI) was drawn in the center of the left ventricular cavity on a midventricular short-axis slice. Thereafter, the number of total ROI counts was noted and the ROI was moved to the hottest area of the left ventricular wall using overrange blank for identification. The ratio of the counts in the two ROIs (cavity and myocardial wall) was calculated and defined as the C/M ratio. The whole procedure was independently performed by two experienced observers blind to the other patient's data. Intraobserver variability was assessed by comparing two separate C/M calculations performed blindly by the same observer after a monthly interval.

L/H Ratio

The L/H ratio on the resting ^{99m}Tc-sestamibi images was calculated according to the technique described by Giubbini et al. (*11*). Briefly, the highest counting rate in the cardiac region was automatically identified on the anterior projection and on those immediately preceding and after it. The operator outlined a second circular ROI on the hottest area of the left lung at a distance of at least five pixel from the cardiac region. The average pixel counts of the two regions were measured, and the means of the values in the three projections were used to calculate the L/H ratio.
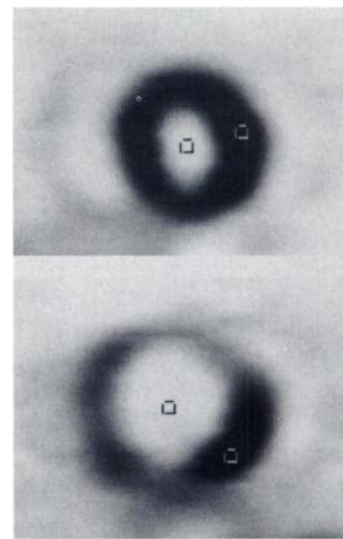
Statistical Analysis

Data are expressed as the mean ± s.d. The comparisons between the various subsets of patients were made using the unpaired Student's t-test with the Bonferroni correction for multiple comparisons. The relationship between C/M ratio, LVEF and LVEDD was assessed with stepwise multiple regression. The reproducibility of the C/M ratio calculation, the relationship between L/H ratio and LVEF, and that between logarithmic transform of the C/M ratio and LVEF and LVEDD were evaluated using the linear regression and Pearson's r coefficient. The capacity of the C/M ratio and of the L/H ratio in differentiating between normal and abnormal LVEF were evaluated using different cutoff values and receiver operating characteristic (ROC) curve analysis. Wilcoxon statistics were used to assess significance of differences between ROC curve areas (*16*). Sensitivity, specificity and accuracy were defined as usual.

RESULTS

General Findings

Of the 95 enrolled patients, coronary artery disease was already known to be present in 48 patients because of documented prior myocardial infarction. In 29 patients, the diagnosis of coronary artery disease was made on the basis of stress-induced perfusion abnormalities and later confirmed by coronary angiography. In the remaining 18 patients, the presence of coronary artery disease was excluded by the results of multiple noninvasive tests and/or by coronary angiography. Forty-eight patients had a normal LVEF (mean 59.8% ± 4%, range 50%–67%) and 47 had abnormal values (36% ± 8%, range 18%–49%). A clearly enlarged left ventricle (LVEDD ≥ 58 mm) was detected in 20 patients who all had an abnormal LVEF (*15*).
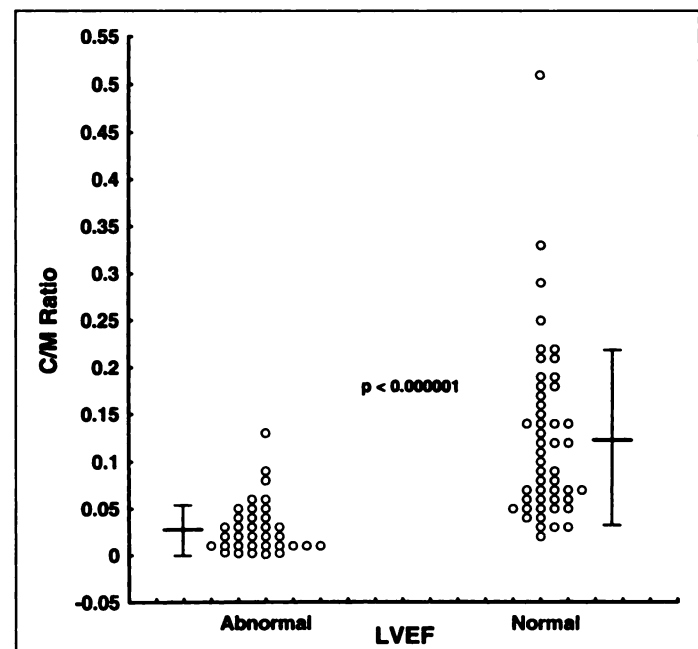

FIGURE 1. Examples of ROI identification for C/M ratio calculation in a patient with normal LVEF and LVEDD (top) and in a patient with severely depressed LVEF and an enlarged left ventricle (bottom).

C/M Ratio

Examples of ROIs for C/M ratio calculation are shown in Figure 1. Both the intra- and the interobserver variability of the C/M ratio calculation were acceptable: r = 0.96 and r = 0.95, respectively (both p < 0.00001). In a subset of 30 patients, the C/M ratio was also calculated on the images obtained after 1 hr of pharmacologic stress testing: a high correlation (r = 0.97, p < 0.000001) with the related value calculated on the rest images was observed. The mean C/M ratio of the whole population was 0.076 ± 0.084, range 0.001–0.51. The 47 patients with depressed LVEF had significantly lower C/M ratio values (0.026 ± 0.028) than the patients with normal LVEF (0.125 ± 0.093) (p < 0.000001) (Fig. 2). Similarly, the 20 patients with increased LVEDD had significantly lower C/M ratio (0.023 ± 0.027) than the 75 patients with normal LVEDD (0.09 ± 0.089, p < 0.005).

To define which parameter determined the C/M ratio, stepwise multiple regression was performed using the C/M ratio as

FIGURE 2. Distribution of C/M ratio in patients with abnormal or normal LVEF. Individual data points and mean value ± s.d. are shown.

TABLE 1
Results of Stepwise Multiple Regression for C/M Ratio

Step	Variable	Multiple R	F to enter	p value
1	LVEF	0.76	134.3	<0.000001
2	LVEDD	0.81	17.4	<0.0001

dependent and LVEF and LVEDD as independent variables. Both LVEF and LVEDD showed a significant correlation with C/M (Table 1). The correlation between LVEF and C/M ratio was r = 0.6, p < 0.000001 and that between LVEDD and C/M ratio was r = −0.51, p < 0.00001. However, the point distribution suggested that both relationships were not linear (Figs. 3 and 4). Therefore, to verify whether it was possible to predict LVEF or LVEDD values starting from the C/M ratio, linearization was attempted by using the natural logarithm transform of the C/M ratio as an independent variable. The derived relationships appeared to be linear and allowed a reasonable prediction of the LVEF (r = 0.73, p < 0.000001, s.e.e. = 9.26) (Fig. 5) and LVEDD (r = −0.6, p < 0.000001, s.e.e. = 5.6) (Fig. 6).

L/H Ratio

The mean L/H ratio of the patient population was 0.48 ± 0.09. A significantly higher value was observed in the 47 patients with abnormal LVEF compared to those with normal function: 0.53 ± 0.09 versus 0.43 ± 0.06, p < 0.00001. The correlation between L/H ratio and resting LVEF was r = −0.42, p < 0.00001.

Detection of Patients with Abnormal LVEF

ROC analysis of the C/M ratio, using various possible cutoff points to differentiate patients with normal and abnormal LVEF is shown in Figure 7. The ROC curve area was 0.89 ± 0.03. Using the optimal cutoff point (LVEF abnormal with C/M ratio < 0.07), 44 of 47 patients with abnormal LVEF and 34 of 48 patients with normal function were correctly classified, with 94% sensitivity, 71% specificity and 82% accuracy. The ROC curve for L/H ratio is shown in Figure 8. Its area was 0.79 ± 0.05, p < 0.03 versus C/M ratio area. Using the optimal cutoff value (LVEF abnormal with L/H ratio ≥ 0.455), 41 of 47 patients with abnormal LVEF and 34 of 48 patients with normal function were correctly classified, resulting in 87% sensitivity, 71% specificity and 79% accuracy.
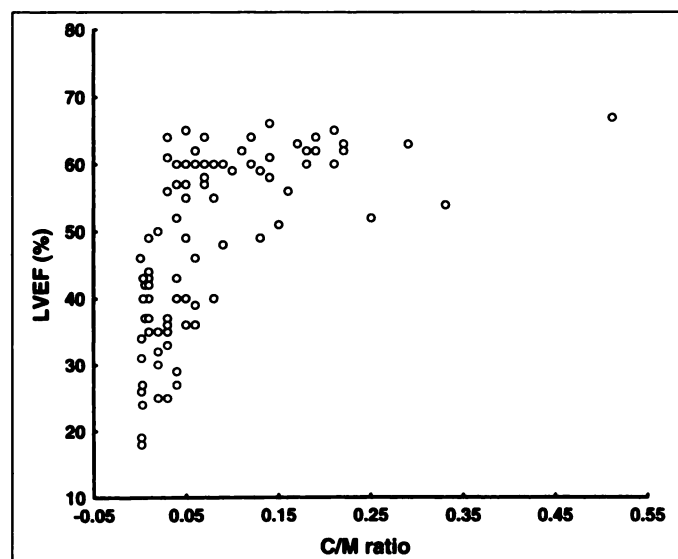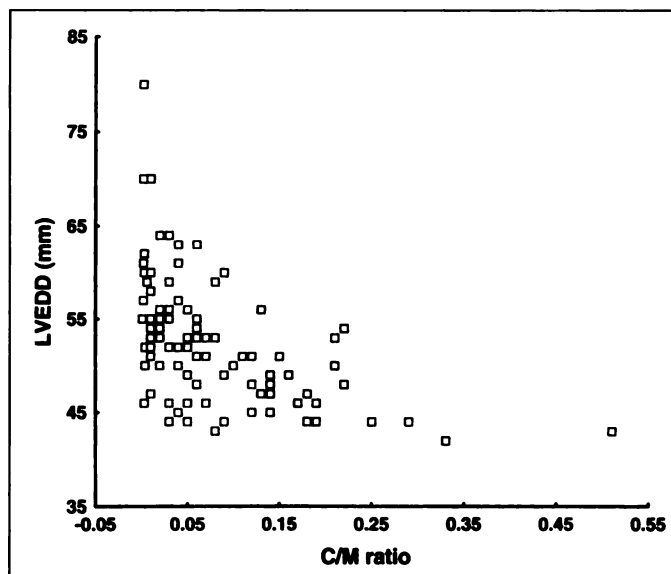

FIGURE 4. Scatterplot of C/M ratio versus LVEDD.

DISCUSSION

This study demonstrates a parameter, the C/M ratio, that can be easily calculated from ^{99m}Tc-sestamibi SPECT images for use in identifying patients with abnormal LVEF directly from the myocardial perfusion images. The common observation that the left ventricular cavity is "emptier" or "darker" on SPECT ^{201}Tl images of patients with poor ventricular function (17) led Roberti et al. (12) to define the C/M ratio as a useful parameter in the estimation of the left ventricular function. The mechanisms which can determine tracer activity in the center of the left ventricular cavity are multiple. They include spillover activity from the myocardial walls, activity from the myocardial wall which overlie and underlie the ventricular cavity en face, activity within the blood pool and effects of Compton scattering and soft-tissue attenuation (12). In patients with depressed left ventricular function, activity in the cavity decreases and hence a lower [201]Tl C/M ratio is detected (12). As expected, our results show that this circumstance is also observed with ^{99m}Tc-sestamibi. However, the several differences between ^{201}Tl and ^{99m}Tc-sestamibi in terms of imaging features and kinetics have to be considered, in that they explain the overall
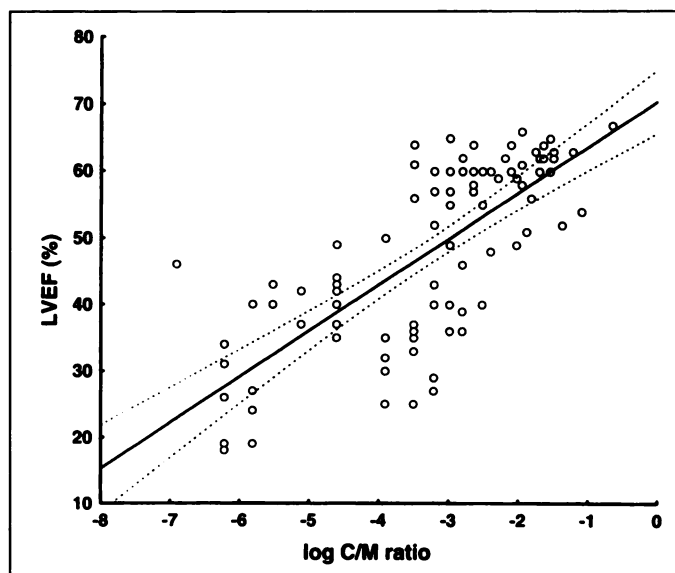

FIGURE 3. Scatterplot of C/M ratio versus LVEF.

FIGURE 5. Scatterplot of natural logarithm of C/M ratio versus LVEF. The regression line and its 95% confidence limits (dotted lines) are shown.
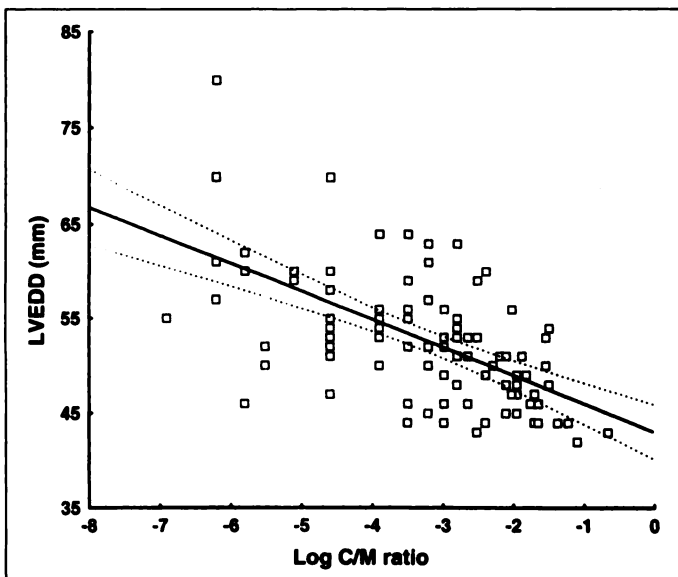
FIGURE 6. Scatterplot of natural logarithm of C/M ratio versus LVEDD. The regression line and its 95% confidence limits (dotted lines) are shown.

lower C/M ratio values we observed with the latter tracer. In particular, the influence of wall activity on cavity counts is limited by the higher resolution and lower attenuation of ^{99m}Tc-sestamibi images and this phenomenon was exalted by the use of a high-resolution collimator and an acquisition zoom (18,19). Consequently, it is not surprising also to have registered a significant inverse relationship between the C/M ratio and LVEDD. In addition, our study included a high percentage of patients with perfusion defects due to prior myocardial infarction, which certainly enhanced the possibility of very poor count recovery in the cavity center. Finally, another factor that possibly contributes to decreased tracer activity in the ventricular cavity is the absence of significant ^{99m}Tc-sestamibi redistribution, which in turn reduces blood-pool activity (1).

The interference of LVEDD and possible infarct perfusion defects on the relationship between the C/M ratio and LVEF makes it difficult to obtain an accurate estimate of LVEF
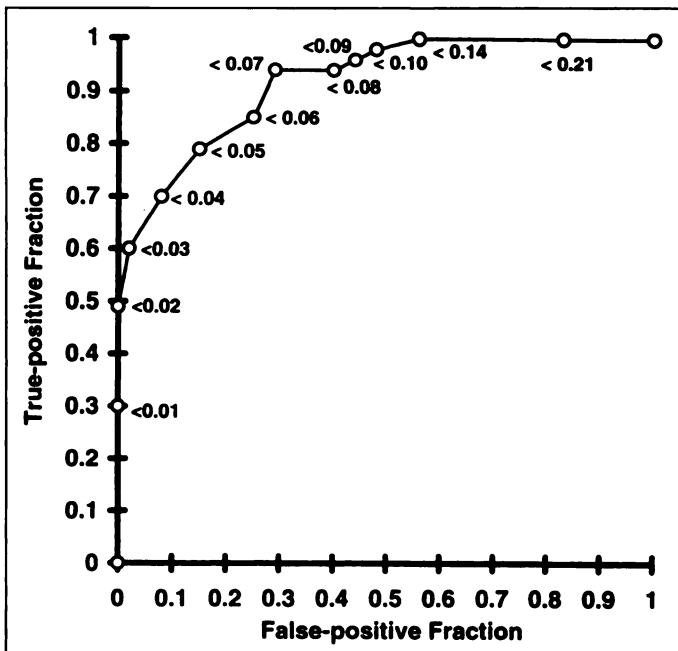

FIGURE 7. ROC curve of the diagnostic accuracy of the C/M ratio to differentiate patients with abnormal and normal resting LVEF.
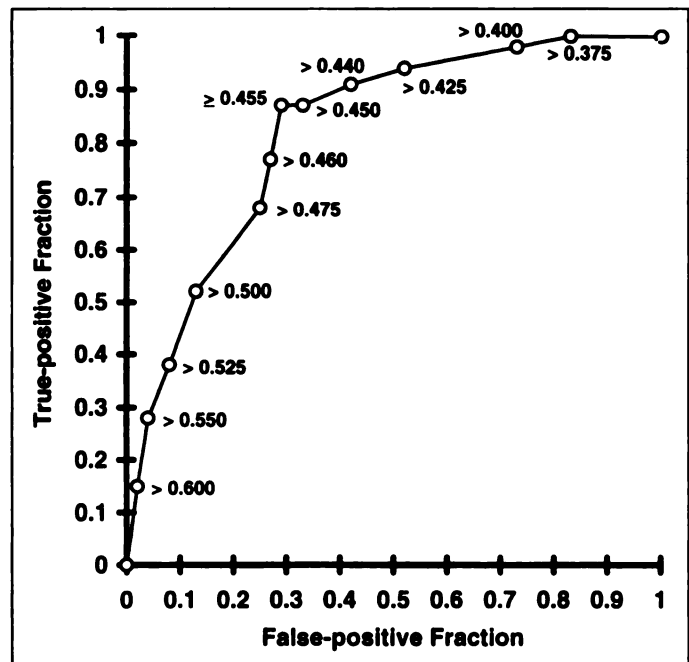

FIGURE 8. ROC curve of the diagnostic accuracy of the L/H ratio to differentiate patients with abnormal and normal resting LVEF.

directly from the C/M ratio. Thus, the method should not be considered as an alternative to direct assessment of LVEF by first-pass radionuclide angiography or gated SPECT. However, despite the apparent influence of LVEDD on the relationship between the C/M ratio and ventricular function, a rough estimate of the LVEF with reasonable error could be achieved from the linear relationship between LVEF and the natural logarithm transform of the C/M ratio. This is not completely unexpected as it is reasonable to assume that the portion of count recovery in a cavity ROI which is caused by attenuation and scatter of myocardial activity, is affected by the distance between ROI and the ventricular wall according to an inverse exponential law (19–21). On the other hand, the main purpose of the C/M ratio was to differentiate patients with depressed left ventricular function from those with normal LVEF. According to our data, the diagnostic accuracy of the C/M ratio to classify left ventricular function as either normal or abnormal does not seem affected by the concomitant effect of ventricular dimensions. Therefore, the same overall diagnostic accuracy achievable with ^{201}Tl could be reached when an appropriate cutoff value was used. It is also remarkable that the C/M ratio was slightly but significantly more effective than the L/H ratio in detecting patients with resting LV dysfunction. Naturally, before using the C/M ratio, each laboratory should identify its own range of normal values to account for the differences in gamma cameras, acquisition modalities and reconstruction procedures.

A major study limitation is the lack of an evaluation of the C/M ratio in the postexercise images and of its relationship with exercise LVEF. The published data on the reliability of postexercise ^{99m}Tc-sestamibi lung uptake could encourage the evaluation of the postexercise C/M ratio (9–11), but the time interval between stress and image acquisition remains a major problem (10). Unfortunately, we were unable to perform this assessment in our population because either only resting images were available or the stress study had been performed using a pharmacologic stimulation. We were only able to demonstrate a close relationship between the C/M ratio calculated on the resting and poststress images in a subgroup of our population. This would imply that the poststress C/M ratio could be used to

estimate resting LVEF if pharmacologic stress has been used and the time interval between stress and SPECT collection is above 1 hr. As for the influence of LVEDD, problems may have arisen if enlarged ventricles with normal function had to be considered, as would have been the care in patients with aortic valve disease. Since there were no patients with significant left ventricular enlargement but normal LVEF in our patient population, no conclusions can be drawn about these subjects.

CONCLUSION

This study demonstrates that the ^{99m}Tc-sestamibi C/M ratio can be used for an approximate assessment of left ventricular function. The accuracy of this parameter in resting ^{99m}Tc-sestamibi SPECT scans appears similar to that reported for ^{201}Tl.

REFERENCES

1. Wackers F, Berman D, Maddahi J, et al. Technetium-99m-hexakis-2-methoxyisobu-tylisonitrile: human biodistribution, dosimetry, safety and preliminary comparison to thallium-201 for myocardial perfusion imaging. *J Nucl Med* 1989;30:301–311.
2. Kiat H, Maddahi J, Roy L, et al. Comparison of technetium-99m-methoxy isobutyl isonitrile and thallium-201 for evaluation of coronary artery disease by planar and tomographic methods. *Am Heart J* 1989;117:1–11.
3. Baillet GY, Mena IG, Kuperus JH, Robertson JM, French WJ. Simultaneous technetium-99m-MIBI angiography and myocardial perfusion imaging. *J Nucl Med* 1989;30:38–44.
4. Bisi G, Sciagrà R, Büll U, et al. Assessment of ventricular function with first-pass radionuclide angiography using technetium-99m-hexakis-2-methoxyisobutylisonitrile: a European multicentre study. *Eur J Nucl Med* 1991;18:178–183.
5. Sciagrà R, Bisi G, Santoro GM, Briganti V, Leoncini M, Fazzini PF. Evaluation of coronary artery disease extent and severity using ^{99m}Tc-sestamibi first-pass and perfusion imaging in combination with dipyridamole infusion. *J Nucl Med* 1994;35:1254–1264.
6. DePuey EG, Nichols K, Dobrinsky C. Left ventricular ejection fraction assessed from gated technetium-99m-sestamibi SPECT. *J Nucl Med* 1993;34:1871–1876.
7. Weiss AT, Berman DS, Lew AS, et al. Transient ischemic dilation of the left ventricle on stress thallium-201 scintigraphy: a marker of severe and extensive coronary artery disease. *J Am Coll Cardiol* 1987;9:752–759.
8. Boucher CA, Zir LM, Beller GA, et al. Increased lung uptake of thallium-201 during exercise myocardial imaging: clinical, hemodynamic and angiographic implications in patients with coronary artery disease. *Am J Cardiol* 1980;46:189–196.
9. Maisey MN, Mistry R, Sowton E. Planar imaging techniques used with technetium-99m-sestamibi to evaluate chronic myocardial ischemia. *Am J Cardiol* 1990;66:47E–54E.
10. Hurwitz GA, Fox SP, Driedger AA, Willems C, Powe JE. Pulmonary uptake of sestamibi on early post-stress images: angiographic relationships, incidence and kinetics. *Nucl Med Commun* 1993;14:15–22.
11. Giubbini R, Campini R, Milan E, et al. Evaluation of technetium-99m-sestamibi lung uptake: correlation with left ventricular function. *J Nucl Med* 1995;36:58–63.
12. Roberti RR, Van Tosh A, Baruchin MA, et al. Left ventricular cavity-to-myocardial count ratio: a new parameter for detecting resting left ventricular dysfunction directly from tomographic thallium perfusion scintigraphy. *J Nucl Med* 1994;34:193–198.
13. Folland ED, Parisi AF, Moynihan PF, Jones DR, Feldman CL, Tow DE. Assessment of left ventricular ejection fraction and volumes by real-time, two-dimensional echocardiography. A comparison of cineangiographic and radionuclide techniques. *Circulation* 1979;60:760–766.
14. Stamm RB, Carabello BA, Mayers DL, Martin RP. Two-dimensional echocardiographic measurement of left ventricular ejection fraction: prospective analysis of what constitutes an adequate determination. *Am Heart J* 1982;104:136–144.
15. Feigenbaum H. Appendix. Echocardiographic measurements and normal values. In: Feigenbaum H, ed. *Echocardiography*, 5th ed. Philadelphia: Lea and Febiger; 1994;658.
16. Hanley JA, McNeil BJ. A method of comparing the areas under receiving operating characteristic curves derived from the same cases. *Radiology* 1983;148:839–843.
17. Civelek AC, Shafique I, Brinker JA, et al. Reduced left ventricular cavity activity ("black hole sign") in thallium-201 SPECT perfusion images of anteroapical transmural myocardial infarction. *Am J Cardiol* 1991;68:1132–1137.
18. Budinger TF, Derenzo SE, Greenberg WL, Gullberg GT, Huesman RH. Quantitative potentials of dynamic emission computed tomography. *J Nucl Med* 1978;19:309–315.
19. Passeri A, Formiconi AR, Meldolesi U. Physical modeling (geometrical system response, compton scattering and attenuation) in brain SPECT using the conjugate gradient reconstruction method. *Phys Med Biol* 1993;38:1727–1744.
20. Axelsson B, Msaki P, Israelsson A. Subtraction of Compton scattered photons in SPECT. *J Nucl Med* 1984;25:490–494.
21. Frey EC, Tsui BMW. Spatial properties of the scatter response function in SPECT. *IEEE Trans Nucl Sci* 1991;NS-38:789–794.

PET Perfusion and Vasodilator Function After Angioplasty for Acute Myocardial Infarction

Richard E. Stewart, D. Douglas Miller, Terry R. Bowers, Peter A. McCullough, Richard A. Ponto, Cindy L. Grines, William W. O'Neill, Jack E. Juni and Robert D. Safian

Division of Cardiology and Nuclear Medicine, William Beaumont Hospital, Royal Oak, Michigan; Division of Cardiology, Department of Internal Medicine, St. Louis University, Health Science Center, St. Louis, Missouri

The aims of this study were to validate invasive coronary Doppler flows against noninvasive PET assessments of myocardial perfusion and to examine the timing and degree of regional coronary vasodilator reserve recovery in patients who are successfully reperfused with primary angioplasty (PTCA) for acute myocardial infarction. **Methods:** PTCA was performed in 21 consecutive patients with acute myocardial infarction; the final diameter stenosis was 25% ± 7%. After restoration of TIMI Grade 3 flow, all patients underwent quantitative coronary angiography and distal Doppler coronary blood flow studies (basal and after adenosine-induced hyperemia) in the infarct and noninfarct vessels. Regional myocardial perfusion and vasodilator function were quantitated after intravenous adenosine infusion PET in all patients at 26 ± 9 hr after acute PTCA. These were repeated in 17 patients 9 ± 3 days later. **Results:** Post-PTCA resting coronary flow was 35 ± 15 ml/min in the infarct-related vessels and 50 ± 24 ml/min during peak hyperemia (p < 0.05). Coronary flow reserve (CFR) was 1.48 ± 0.34 and 2.08 ± 0.62 in the infarct and noninfarct vessels, respectively (p < 0.001). Early (<36 hr) PET myocardial perfusion reserves (MPR) in the infarct and noninfarct regions were 1.59 ± 0.33 and 2.03 ± 0.62 (p < 0.01). Doppler CFR and PET MPR were correlated in the infarct (r = 0.61, p < 0.01) and noninfarct (r = 0.77, p < 0.0001) regions. Follow-up PET studies demonstrated improved MPR in both infarct and noninfarct regions (1.93 ± 0.52 versus 2.54 ± 0.97, p < 0.01). The improvement in coronary vasodilator function from the time of acute PTCA to follow-up PET in the infarct region was significant (p = 0.005). **Conclusion:** After successful mechanical revascularization by PTCA after acute myocardial infarction, intracoronary Doppler blood flows and noninvasive PET regional myocardial perfusion are correlated within the wide range of reperfusion blood flows observed in patients with contrast angiographic TIMI Grade 3 flow. Serial PET studies demonstrated a trend towards continued improvement in the vasodilator response in infarct-related myocardial regions after the restoration of blood flow by PTCA. PET offers the potential for accurate noninvasive serial assessment of reperfusion blood flow after primary angioplasty for acute myocardial infarction.

Key Words: myocardial infarction; coronary flow; angioplasty; PET

J Nucl Med 1997; 38:770–777

The immediate treatment goals for acute myocardial infarction are to re-establish blood flow, salvage myocardium and limit